Contents lists available at SCCE

Journal of Soft Computing in Civil Engineering

Journal homepage: www.jsoftcivil.com

Flexural Analysis of Deep Aluminum Beam

A. Dahake[1*], P. Kapdis[2], U. Kalwane[2], U. Salunkhe[2]

1. Associate Professor and Head, Civil Engineering Department, Maharashtra Institute of Technology, Aurangabad (M. S.), India
2. Civil Engineering Department, Shreeyash College of Engineering and Technology, Aurangabad, (M. S.), India
Corresponding author: *ajaydahake@gmail.com*

https://doi.org/10.22115/SCCE.2018.49679

ARTICLE INFO

Article history:
Received:23 August 2017
Revised: 27 August 2017
Accepted: 28 August 2017

Keywords:
Deep beam;
Deformations;
Deflections;
Aluminum.

ABSTRACT

Many parts of spacecraft, airplanes are made up of aluminum, due to its property of less density, which is deep in sections. For the analysis of deep parts of any structure, a shear deformation theory using the trigonometric sinusoidal function in displacement field in terms of thickness coordinate is developed to obtain the shear deformation effects. The shear stresses are obtained from the use of constitutive equations with outstanding accuracy, satisfying the zero shear stress at the both, top and bottom of beams. Also, the theory not requires the shear correction factor. By using the principle of virtual work, the governing differential equations and boundary conditions are obtained. A deep aluminum beam is assumed subjected to a cosine load for the analytical study to show the accuracy of the theory. The results are compared with other theories.

1. Introduction

Euler-Bernoulli theory disregards the property of the shear deformation and heavy stress concentration hence it is applicable for thin beams only. As the theory neglect the shear

How to cite this article: Dahake A, Kapdis P, Kalwane U, Salunkhe U. Flexural analysis of deep aluminum beam. J Soft Comput Civ Eng 2018;2(1):71–84. https://doi.org/10.22115/scce.2018.49679.

2588-2872/

deformation, and it is more pronounced in the case of deep beams. Hence it is essential to address the shear deformation effects.

Timoshenko [1] considered a prismatic bar to investigate the effect of transverse vibration. This theory is known as first-order shear deformation theory (FSDT) and Timoshenko theory in the literature. The shear strain is assumed to be constant through the thickness of the beam and thus requires shear correction factor.

Cowper [2] has denied an expression for the shear correction factor for various cross-sections of the beam. The discrepancies in the elementary theory of beam and first-order shear deformation theories; various higher order shear deformation theories were developed and available in the literature for static and dynamic analysis of beams. Krishna Murthy [3], Baluch *et al*. [4], A parabolic shear deformation theory is developed by Bhimaraddi and Chandrashekhara [5] assuming a variety of axial displacement. These theories satisfy shear stress conditions on both faces of the beam and thus no need of shear correction factor.

Dahake and Ghugal [6] studied flexural analysis of thick beam having simple supports using trigonometric shear deformation theory. Ghugal and Dahake [7,8] given the flexural solution for the beam subjected to parabolic loading. Sawant and Dahake [9] developed the new hyperbolic shear deformation theory. Chavan and Dahake [10,11] presented clamped-clamped beam using hyperbolic shear deformation theory. The displacement and stresses for the thick beam given by Nimbalkar and Dahake [12].

Jadhav and Dahake [13] presented bending analysis of deep cantilever beam using steel as a material. Manal et al. [14] investigated the deep fixed beams using new displacement field. Patil and Dahake [15] carried out finite element analysis using 2D plane stress elements for the thick beam. Dahake et al. [16] studied the flexural analysis of thick fixed beam subjected to cosine load. Tupe et al. [17] compared various displacement fields for static analysis of thick isotropic beams.

In available research, most of the researchers have used steel as a beam material. As many parts of the spacecraft, airplane structures are made up of aluminum due to its low weight density. In this research, an attempt has been made to analyze the aluminum deep cantilever beam subjected to cosine load.

2. Development of theory

The assumed beam is made up of homogeneous and isotropic material which occupies in $0-x-y-z$ the Cartesian coordinate system the region:

$$0 \le x \le L \; ; \quad 0 \le y \le b \; ; \quad -h/2 \le z \le h/2$$

where x, y, z = Cartesian coordinates,

L, b = length, and width of the beam in the x and y directions, respectively, and

h = thickness of the beam in the z-direction.

2.1 Displacement field used

The displacement field used as follows:

$$u(x,z) = -z\left(\frac{dw}{dx}\right) + \frac{h}{\pi}\left[\sin\frac{\pi z}{h}\phi(x)\right] \quad and \; w(x,z) = w(x) \tag{1}$$

Where, u and w = axial and transverse displacements respectively.

Plane strain

$$\varepsilon_x = \frac{\partial u}{\partial x} = -z\frac{d^2 w}{dx^2} + \frac{h}{\pi}\sin\frac{\pi z}{h}\frac{d\phi}{dx} \tag{2}$$

Shear strain

$$\gamma_{zx} = \frac{\partial u}{\partial z} + \frac{dw}{dx} = \cos\frac{\pi z}{h}\phi \tag{3}$$

Stress-Strain Relationships

$$\begin{aligned} \sigma_x &= E\varepsilon_x \\ \tau_{zx} &= G\gamma_{zx} \end{aligned} \tag{4}$$

2.2. Boundary conditions and governing equations

The variationally consistent governing differential equations and boundary conditions for the beam under consideration are mentioned below using the expressions for strains and stresses (2) through (4) and using the principle of virtual work; it leads to:

$$b\int_{x=0}^{x=L}\int_{z=-h/2}^{z=+h/2}\left(\sigma_x \delta\varepsilon_x + \tau_{zx}\delta\gamma_{zx}\right)dx\,dz - \int_{x=0}^{x=L} q(x)\,\delta w\,dx = 0 \tag{5}$$

Where, δ = variational operator.

Employing Green's theorem in Eqn. (4) successively, we obtained the coupled Euler-Lagrange equations which are the governing differential equations and associated boundary conditions of the beam.

$$EI\ \frac{d^4w}{dx^4} - \frac{24}{\pi^3}\ EI\,\frac{d^3\phi}{dx^3} = q(x) \tag{6}$$

$$\frac{24}{\pi^3}\ EI\ \frac{d^3w}{dx^3} - \frac{6}{\pi^2}\,EI\ \frac{d^2\phi}{dx^2} + \frac{GA}{2}\phi = 0 \tag{7}$$

Moreover, associated consistent natural boundary conditions obtained are as follows:

At $x = 0$ and $x = L$

$$EI\frac{d^2w}{dx^2} = EI\frac{d\phi}{dx} = w = 0 \tag{8}$$

2.3. General solution of equilibrium equations

Using Eqns. (6) and (7), we get $w(x)$ and $\phi(x)$

$$\frac{d^3w}{dx^3} = \frac{24}{\pi^3}\frac{d^2\phi}{dx^2} + \frac{Q(x)}{EI} \tag{9}$$

where $Q(x)$ = generalized shear force for beam.

The second governing Eqn. (7) is also rearranged as follows:

$$\frac{d^3w}{dx^3} = \frac{\pi}{4}\frac{d^2\phi}{dx^2}\ - \beta\phi \tag{10}$$

Using Eqns. (11) and (12), we obtained ϕ as:

$$\frac{d^2\phi}{dx^2} - \lambda^2\phi = \frac{Q(x)}{\alpha EI} \tag{11}$$

where constants α, β and λ in Eqns. (10) and (11) are as follows

$$\alpha = \left(\frac{\pi}{4} - \frac{24}{\pi^3}\right),\ \beta = \left(\frac{\pi^3}{48}\frac{GA}{EI}\right) \text{and } \lambda^2 = \frac{\beta}{\alpha}$$

The general solution of Eqn. (11) is obtained as follows:

$$\phi(x) = C_2\cosh\lambda x + C_3\sinh\lambda x - \frac{Q(x)}{\beta EI} \tag{12}$$

The equation of $w(x)$ is obtained by substituting the expression of $\phi(x)$ in Eqn. (12) and then integrating it thrice with respect to x.

The solution for $w(x)$ is obtained as follows:

$$EI\,w(x)=\iiiint q\,dx\,dx\,dx\,dx+\frac{C_1x^3}{6}+\left(\frac{\pi}{4}\lambda^2-\beta\right)\frac{EI}{\lambda^3}\left(C_2\sinh\lambda x+C_3\cosh\lambda x\right)+C_4\frac{x^2}{2}+C_5x+C_6 \tag{13}$$

where, C_1, C_2, C_3, C_4, C_5 and C_6 are arbitrary constants and can be obtained by imposing natural (static) and / or geometric or kinematical end conditions of the beam.

3. Illustrative example

To establish the effectiveness of the theory, a numerical example is assumed. For the static a rectangular deep cross-section, having span '*L*', width '*b*' and thickness '*h*' of elastic material is considered. The following material properties for beam are used.

Table 1
Properties of aluminum 6061-T6, 6061-T651 [18].

Physical Properties	**Quantity**
Density	2700 kg/m^3
Ultimate Tensile Strength	310 MPa
Modulus of Elasticity	68.9 GPa
Notched Tensile Strength	324 MPa
Ultimate Bearing Strength	607 MPa
Bearing Yield Strength	386 MPa
Poisson's Ratio	0.33

3.1. Example: A clamped beam subjected to cosine load

The beam has its origin at $x = 0$ and free at $x = L$. The load acting as shown in Fig. 2, on surface $z = +h/2$ acting in the downward z-direction.

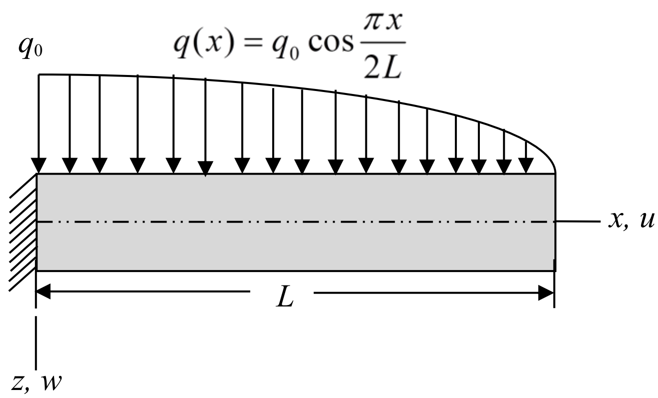

Fig. 2. Beam subjected to cosine load.

Associated boundary conditions for the above beam are:

At free end: $EI\frac{d^2w}{dx^2} = EI\frac{d\phi}{dx} = EI\frac{d^3w}{dx^3} = EI\frac{d^2\phi}{dx^2} = 0$ at $x = L$

and at fixed end: $\frac{dw}{dx} = \phi = w = 0$ at $x = 0$

The expressions obtained in general form for $w(x)$ and $\phi(x)$ are as:

$$w(x) = \frac{q_0 L^4}{120EI}\left\{\begin{array}{l} -\frac{960}{\pi^3}\left[-\frac{2}{\pi}\left(\cos\frac{\pi x}{2L} - 1\right) - \frac{1}{2}\frac{x^2}{L^2}\right] - \frac{4920}{\pi^4}\left(\frac{1}{6}\frac{x^3}{L^3} - \frac{1}{4}\frac{x^2}{L^2}\right) \\ -\frac{240}{\pi^3}\frac{E}{G}\frac{h^2}{L^2}\left[-\frac{2}{\pi}\left(\cos\frac{\pi x}{2L} - 1\right) - \frac{1}{2}\frac{x^2}{L^2}\right] \\ -5\frac{E}{G}\frac{h^2}{L^2}\left(-\frac{x}{L} - \frac{1}{2}\frac{x^2}{L^2} + \frac{\sinh\lambda x - \cosh\lambda x + 1}{\lambda L}\right) \end{array}\right\} \tag{14}$$

$$\phi(x) = \frac{q_0 L}{\beta EI}\left(1 - \frac{2\pi^3}{41}\sin\frac{\pi x}{2L} + \sinh\lambda x - \cosh\lambda x\right) \tag{15}$$

The stresses and axial displacement are obtained using the above solutions are as follows

$$u=\frac{q_0 h}{Eb}\left[\begin{array}{l}-\frac{1}{10}\frac{z}{h}\frac{L^3}{h^3}\left(\begin{array}{l}-31\left(\sin\frac{\pi x}{2L}-\frac{x}{L}\right)-8\frac{E}{G}\frac{h^2}{L^2}\left(\sin\frac{\pi x}{2L}-\frac{x}{L}\right)\\-5\frac{E}{G}\frac{h^2}{L^2}\left(\frac{x}{L}-1+\cosh\lambda x-\sinh\lambda x\right)-51\left(\frac{1}{2}\frac{x^2}{L^2}-\frac{1}{2}\frac{x}{L}\right)\end{array}\right)\\-\frac{104}{5\pi^4}\sin\frac{\pi z}{h}\frac{E}{G}\frac{L}{h}\left(\frac{30}{13}\frac{x}{L}-\frac{10}{13}\frac{x^3}{L^3}-1+\cosh\lambda x-\sinh\lambda x\right)\end{array}\right] \tag{16}$$

$$\sigma_x=\frac{q_0}{b}\left[\begin{array}{l}-\frac{1}{10}\frac{z}{h}\frac{L^2}{h^2}\left(\begin{array}{l}60\frac{x^2}{L^2}-10\frac{x^4}{L^4}+8-52\frac{x}{L}-\frac{12}{\pi^2}\frac{E}{G}\frac{h^2}{L^2}\left(-\frac{x^2}{L^2}+\frac{1}{3}\right)\\-\frac{26}{5}\frac{E}{G}\frac{h^2}{L^2}\left(1+\lambda L(\sinh\lambda x-\cosh\lambda x)\right)\end{array}\right)\\-\frac{104}{5\pi^4}\sin\frac{\pi z}{h}\frac{E}{G}\left(\frac{30}{13}-\frac{30}{13}\frac{x^2}{L^2}+\lambda L(\sinh\lambda x-\cosh\lambda x)\right)\end{array}\right] \tag{17}$$

$$\tau_{zx}^{CR}=\frac{104}{5\pi^3}\frac{q_0}{b}\frac{L}{h}\cos\frac{\pi z}{h}\left(1+\frac{10}{13}\frac{x^3}{L^3}-\frac{30}{13}\frac{x}{L}+\sinh\lambda x-\cosh\lambda x\right) \tag{18}$$

$$\begin{aligned}\tau_{zx}^{EE}=&\frac{q_0 L}{80bh}\left(4\frac{z^2}{h^2}-1\right)\left[40\frac{x^3}{L^3}-4-\frac{240}{\pi^2}\frac{x}{L}-\frac{4}{5}\frac{E}{G}\frac{h^2}{L^2}\lambda^2L^2\left(\cosh\lambda x-\sinh\lambda x\right)\right]\\&-\frac{16}{5\pi^5}\cos\frac{\pi z}{h}\frac{E}{G}\frac{q_0 h}{bL}\left[-1+5\frac{x^3}{L^3}+\lambda^2L^2\left(\cosh\lambda x-\sinh\lambda x\right)\right]\end{aligned} \tag{19}$$

4. Results

4.1. Numerical Results

In the present research, the results for displacements, (axial, transverse and inplane) also, stresses are investigated. The results are presented in the non-dimensional form.

$$\bar{u}=\frac{Ebu}{q_0 h},\quad \bar{w}=\frac{10Ebh^3 w}{q_0 L^4},\quad \bar{\sigma}_x=\frac{b\sigma_x}{q_0},\quad \bar{\tau}_{zx}=\frac{b\tau_{zx}}{q_0}$$

The shear stresses ($\bar{\tau}_{zx}$) are obtained directly by using constitutive relation and equilibrium equation of two-dimensional elasticity and are denoted by ($\bar{\tau}_{zx}^{CR}$) and ($\bar{\tau}_{zx}^{EE}$) respectively. It satisfies the stress-free conditions on the top $(z=-h/2)$ and bottom $(z=+h/2)$ faces of the beam.

Table 2

Axial Displacement ($\bar{u}$) at ($x = L, z = h/2$), Deflection ($\bar{w}$) at ($x = L, z = 0.0$) Bending Stress ($\bar{\sigma}_x$) at ($x = 0, z = h/2$), Shear Stresses $\bar{\tau}_{zx}^{CR}$ (x=0.01L, z = 0) and $\bar{\tau}_{zx}^{EE}$ (x, z = 0) of the Beam for Aspect Ratio 4 and 10.

Source	Aspect ratio	Model	$\bar{u}$	$\bar{w}$	$\bar{\sigma}_x$	$\bar{\tau}_{zx}^{CR}$	$\bar{\tau}_{zx}^{EE}$
Present		TSDT	-67.5989	6.1819	36.7529	1.8181	-2.7877
Sawant and Dahake [9]		HPSDT	-70.024	6.1928	39.8104	2.1609	-4.5581
Krishna Murty[3]	4	HSDT	-71.2291	6.1860	37.2887	1.9004	-2.8916
Timoshenko [1]		FSDT	23.1543	6.5444	22.2081	0.3076	3.7597
Bernoulli-Euler		ETB	23.1543	5.7541	22.2081	—	3.7597
Present		TSDT	-1055.4548	5.8244	176.7877	7.7501	3.2052
Sawant and Dahake [9]		HPSDT	-1061.5175	5.8256	178.4137	8.3023	3.8042
Krishna Murty[3]	10	HSDT	-1064.5122	5.8255	172.1017	7.8208	3.7523
Timoshenko [1]		FSDT	361.7856	5.8805	138.8010	4.8073	9.3993
Bernoulli-Euler		ETB	361.7856	5.7541	138.8010	—	9.3993

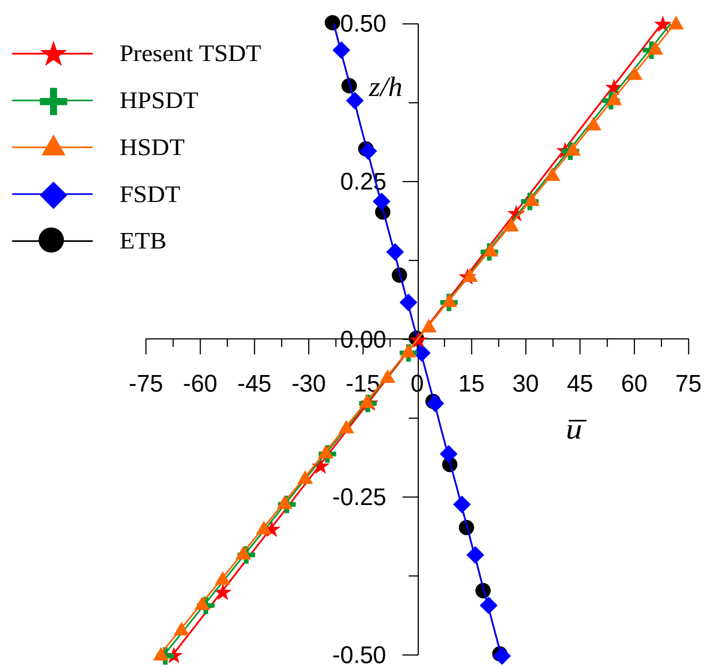

Fig. 2. Variation of $\bar{u}$ through the thickness of the beam for aspect ratio 4.

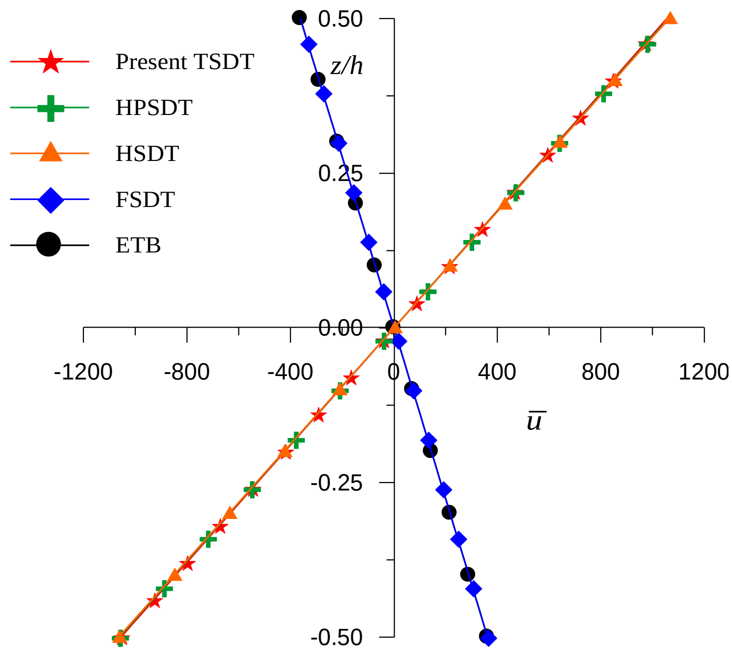

Fig. 3. Variation of $\bar{u}$ through the thickness of the beam for aspect ratio 10.

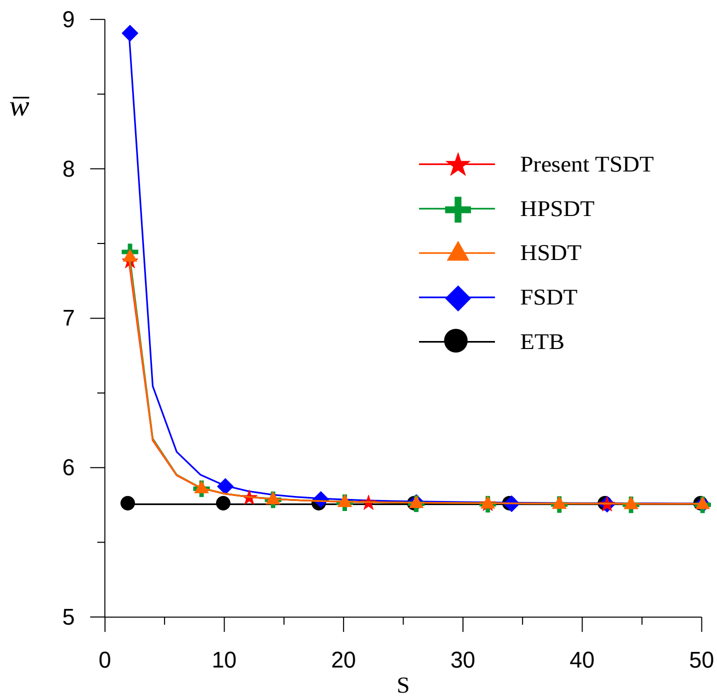

Fig. 4. Variation of a maximum $\bar{w}$ of the beam with aspect ratio *S*.

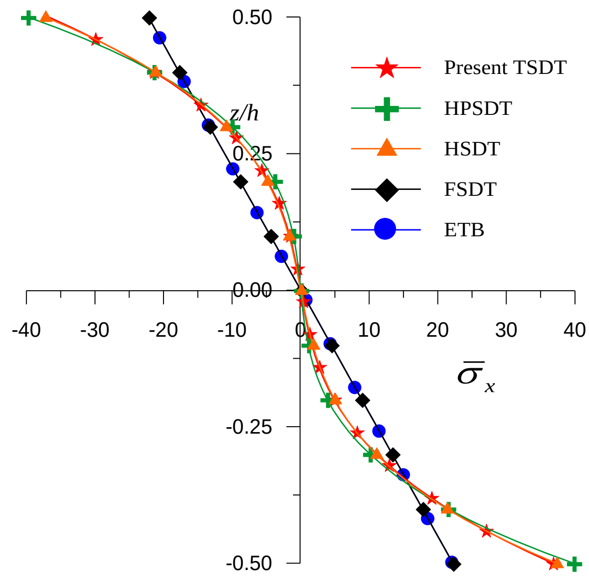

Fig. 5. Bending stress ($\overline{\sigma}_x$) through the thickness at (x= 0, z) for aspect ratio 4.

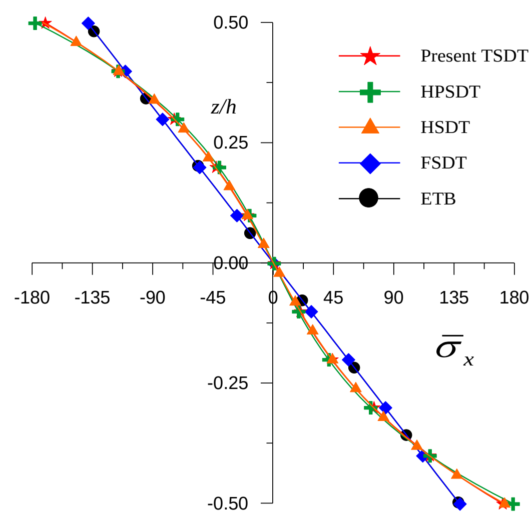

Fig. 6. Bending stress ($\overline{\sigma}_x$) through the thickness at (x= 0, z) for aspect ratio 10.

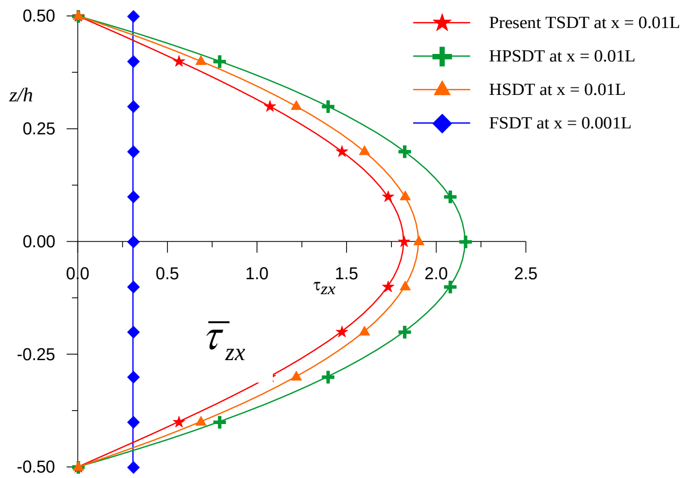

Fig. 7. Shear stress ($\overline{\tau}_{zx}$) through the thickness at (x = 0.01L, z) obtain using CR for aspect ratio 4.

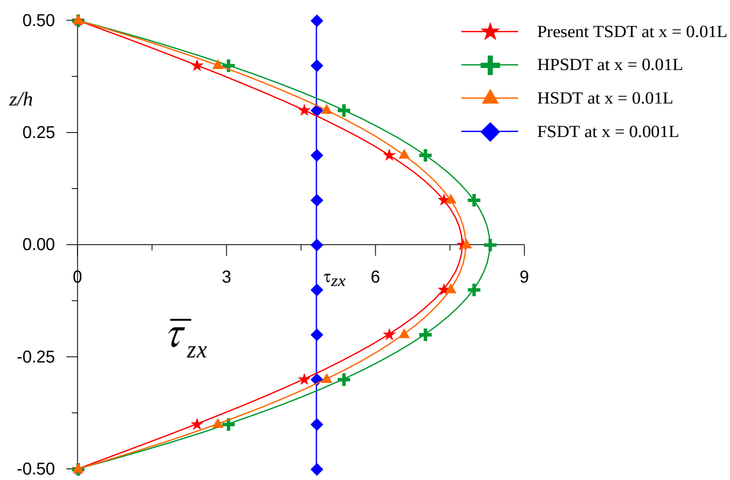

Fig. 8. Shear stress ($\overline{\tau}_{zx}$) through the thickness at (x = 0.01L, z) obtain using CR for aspect ratio 10.

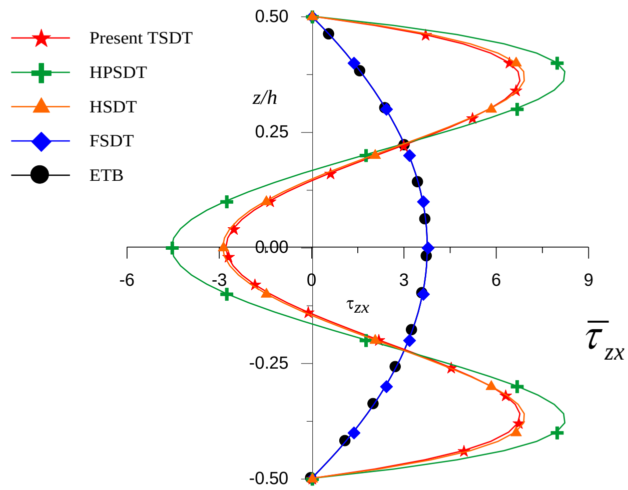

Fig. 9. Shear stress ($\overline{\tau}_{zx}$) through the thickness at (x = 0.01L, z) obtain using EE for aspect ratio 4.

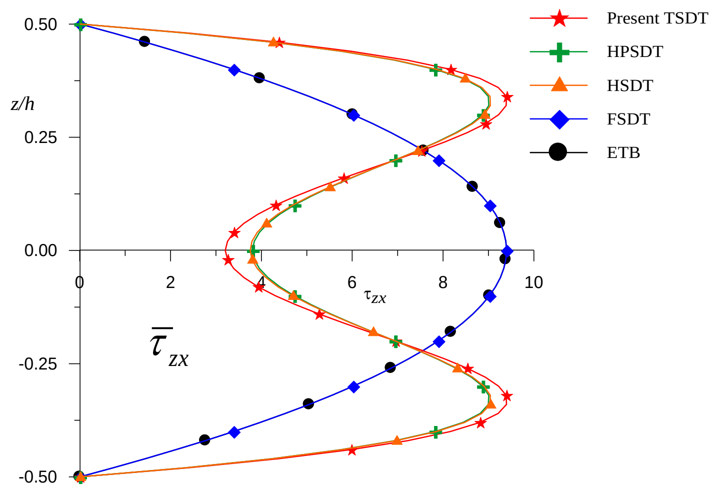

Fig. 10. Shear stress ($\overline{\tau}_{zx}$) through the thickness of beam at (x = 0, z) obtain using EE for aspect ratio 10.

5. Conclusions

The theory gives reasonable results of this component in the displacement field in proportionate with various shear deformation theories. The transverse deflection given is in good agreement with that of other higher order shear deformation theories. The flexural stress and its distribution across the thickness given by theory are in very good agreement with that of higher order shear deformation theories. Also, the for a cantilever beam with cosine load, transverse shear stress and its distribution through the thickness of beam obtained using constitutive relation is in close agreement with that of other higher order refined theories; however, it cannot predict the effect of stress concentration at the built-in end of the beam. By using the equilibrium equation of two-dimensional elasticity, the effect of stress concentration is exactly predicted.

References

[1] Timoshenko SP. LXVI. On the correction for shear of the differential equation for transverse vibrations of prismatic bars. London, Edinburgh, Dublin Philos Mag J Sci 1921;41:744–6. doi:10.1080/14786442108636264.

[2] Cowper GR. The Shear Coefficient in Timoshenko's Beam Theory. J Appl Mech 1966;33:335. doi:10.1115/1.3625046.

[3] K MA V. Vibration of Short Beams. AIAA J 1970;8:34–8.

[4] Baluch MH, Azad AK, Khidir MA. Technical Theory of Beams with Normal Strain. J Eng Mech 1984;110:1233–7. doi:10.1061/(ASCE)0733-9399(1984)110:8(1233).

[5] Bhimaraddi A, Chandrashekhara K. Observations on Higher-Order Beam Theory. J Aerosp Eng 1993;6:408–13. doi:10.1061/(ASCE)0893-1321(1993)6:4(408).

[6] Dahake AG, Ghugal YM. Flexure of Thick Simply Supported Beam Using Trigonometric Shear Deformation Theory. Int J Sci Res Publ 2012;2:1–7.

[7] Ghugal YM, Dahake AG. Flexural analysis of deep beam subjected to parabolic load using refined shear deformation theory. Appl Comput Mech 2012;6:163–72.

[8] Ghugal YM, Dahake AG. Flexure of thick beams using refined shear deformation theory. Int J Civ Struct Eng 2012;3:321–35.

[9] Sawant MK, Dahake AG. A new hyperbolic shear deformation theory for analysis of thick beam. Int J Innov Res Sci Eng Technol 2014;3:9634–43.

[10] Chavan VB, Dahake AG. Analysis of Thick Beam Bending Problem by Using a New Hyperbolic Shear Deformation Theory. Int J Eng Res Gen Sci 2014;2:209–15.

[11] B. C V., G. DA. A Refined Shear Deformation Theory for Flexure of Thick Beam. Int J Pure Appl Res Eng Technol 2015;3:109–19.

[12] Nimbalkar VN, Dahake AG. Displacement and Stresses for Thick Beam using New Hyperbolic Shear Deformation Theory. Int J Pure Appl Res Eng Technol 2015;4:120–30.

[13] Jadhav VA, Dahake AG. Bending Analysis of Deep Beam Using Refined Shear Deformation Theory. Int J Eng Res 2016;5:526–31.

[14] S. MS, M. SR, G. DA. A New Trigonometric Shear Deformation Theory for Thick Fixed Beam. Int J Eng Res 2016;5:532–6.

[15] B. PP, G. DA. Finite Element Analysis Using 2D Plane Stress Elements for Thick Beam. J Aerosp Eng Technol 2016;6:1–8.

[16] G. DA, S. MS, M. SR. Flexure of Fixed Thick Beam using Trigonometric Shear Deformation Theory. Proc. 6th Int. Congr. Comput. Mech. Simulation, Indian Inst. Technol. Powai Maharashtra, India, 2016, p. 1112–5.

[17] A.G. Dahake D. H. Tupe GRG. COMPARISON OF VARIOUS DISPLACEMENT FIELDS FOR STATIC ANALYSIS OF THICK ISOTROPIC BEAMS. Struct. Eng. Conv. CSIR-SERC, Chennai, INDIA. 21-23, 2016, p. 468–72.

[18] Properties of Aluminum 6061-T6, 6061-T651 n.d. http://www.aerospacemetals.com.